JOURNAL OF CATALYSIS 29, 224–245 (1973)

Growth Kinetics and the Size Distributions of Supported Metal Crystallites

E. RUCKENSTEIN AND B. PULVERMACHER

Department of Chemical Engineering, University of Delaware, Newark, Delaware 19711

Received September 22, 1972

Aging kinetics of supported metal catalysts are represented by a model accounting for diffusion of crystallites on the support and sintering of the colliding crystallites. Equations are established for the time dependence of the distribution of crystallite sizes and for the decay of the exposed surface area of metal for both homogeneous and nonhomogeneous surfaces. For homogeneous surfaces the size distribution becomes after a certain time almost independent of the initial distribution and can be represented by a universal curve. On the basis of the universal curve simple decay equations for the exposed surface area of metal (S) are obtained. For nonhomogeneous surfaces having some sites which interact strongly with crystallites an equilibrium size distribution is reached.

The effect of temperature is accounted for by interactions between the metal and support. At high temperatures, the mobility of the crystallites on the support is relatively great and the sintering process is rate determining. At lower temperatures the aging process is diffusion controlled.

The atmosphere affects the aging process by influencing the surface free energies and hence the work of adhesion and the wetting angle between the crystallites and support. If the wetting angle is decreased the mobility of the crystallites is decreased.

Considerations based on surface chemistry are used to suggest possibilities for increasing the stability of the highly dispersed state of metal. For example, stability may be increased if certain alloys are used rather than pure metals.

INTRODUCTION

The degree of dispersion of a metal on a support affects both the activity and selectivity of the supported metal catalyst. In freshly prepared catalyst the metal is generally highly dispersed so that a large fraction of the metal atoms are accessible to reactants. Deactivation and aging, observed after excessive heating (*1–7*) or use under industrial conditions (*5, 7, 8*), are associated with aggregation and sintering of the small crystallites. For example, Herrmann *et al.* (*6*) and Maat and Moscou (*1*) observed that heat treatment of a highly dispersed supported platinum catalyst caused the formation and growth of platinum crystallites and thus a decay of the exposed surface area of the metal.

Analyzing the available experimental data (*1, 3, 6, 7*), described below in some detail, we have observed that the rate of decay of exposed surface area of metal is given by an equation of the form

$$\frac{dS}{dt} = -KS^n, \qquad (1)$$

where the exponent n has a lower bound of about 2 and an upper bound as large as 8. The large range in the value of the exponent suggests that more than one process is responsible for the decay of the exposed surface area of metal.

Several models have been developed by

the authors (*9*) to describe the aging process caused by thermal treatment. The models assume (a) diffusion of the crystallites upon the surface of the support and (b) sintering of the colliding particles. Quantitative descriptions of the decay of the exposed surface area have been obtained in particular in the two limiting cases of diffusion and sintering control. For sintering control the value of n is about 2, while for diffusion control it may be as large as 8.

The goals of the present research are: (a) from the proposed models to obtain information concerning the size distribution of the metal crystallites for various possible mechanisms and to compare the distribution with available experimental data; (b) to obtain additional information concerning the rate of decay of the exposed metal surface area and to relate the exponent n from Eq. (1) to the mechanism of the aging process; (c) to suggest explanations for the effects of the atmosphere on the aging process; (d) to explain the effect of the method of preparation of the supported metal catalyst on the aging process; (e) to suggest possible ways to increase the life (stability) of the small crystallites.

In the first section of the paper the main results of our previous paper are reviewed and further arguments supporting the physical models are presented. Some modification of the earlier models are added which take into account the nonhomogeneity of the surface of the support. Subsequently the time evolution of the size distribution and of the exposed surface area are analyzed. There follows a detailed comparison between theory and experiment concerning both the time decay of the exposed surface area of metal and the size distribution of the metal crystallites. Finally possible improvements of the stability of the highly dispersed state of the metal are suggested.

Physical Model and Kinetic Equations

The physical model is based upon the assumptions of (a) diffusion of the crystallites upon the surface of the support and (b) sintering of the colliding particles.

We consider an initially highly dispersed state of metal on the surface of the support, assumed for simplicity to be planar and energetically homogeneous. For sufficiently high temperatures the agglomerates of metal atoms have some mobility on the surface of the support. Indeed, Bassett (*10, 11*), using electron microscopy and a high-vacuum system, observed translation of copper and silver islands on amorphous carbon and graphite and rotation as well as translation of silver islands on a molybdenite support at temperatures as low as 525 K. Skofronick *et al.* (*12, 13*) observed motion and coalescence of gold islands on amorphous supports of carbon and silicon in the temperature range 500 to 700 K. They found that the number of islands per unit surface area decreased with time and that their mean radius increased.

Crystallites of supported catalysts are of the order of 10 to 100 Å in diameter, about the same size as the agglomerates in the above-mentioned experiments. Consequently the assumption that the crystallites migrate on the surface of the support has experimental confirmation.

Alternative mechanisms of mass transfer by which growth of the crystallites might occur are (a) atomic breakup of the crystallites with consecutive migration of the atoms over the support and (b) evaporation of the metal with consecutive vapor phase transport. Since the bonding energies of metal atoms to metal crystallites are much larger than the bonding energies of metal atoms to nonmetallic supports, dissociation of metal atoms is unlikely (*13, 18*).* Evaporation rates of metal have been measured and found to be several orders of magnitude too low to account for the observed growth of the metal crystallites (*5, 13*).

The following treatment emphasizes situations in which sintering of the support

* There are special conditions under which breakup of crystallites with consecutive migration of the formed particles can take place. This problem, of particular interest in the regeneration of catalysts, is discussed briefly in the last section of the paper and will be examined more fully in another paper.

is of secondary importance. That such an assumption can be made, at least in a dry atmosphere, is shown for instance in references (*14*, *15*).

The decay process is thus a consequence of the migration of crystallites on the support surface. Though the detailed mechanism of this migration is not known, it is clear that it is induced by the thermal motion of the atoms at the metal–support interface. Because of the random character of these thermal motions it is reasonable to represent the motion of the crystallites upon the surface of the support by a diffusional model.

When two crystallites collide, two limiting situations can occur. In one of them the interaction between the colliding particles is so strong that they form a single unit within a time which is short compared to the diffusional time. The rate of sintering is in this case diffusion controlled. If the time of the merging process of the colliding particles into a single unit is long compared to the diffusional time, then the merging process is the rate-determining step. For such a situation the name "sintering control" will be used.

Only the main results of the analysis (*9*) based on the above-mentioned assumptions will be given here. Because only binary collisions are important, the number of crystallites per unit surface area of support composed of k metal units, N_{v_k}, increases by collisions of particles composed of i and $k - i$ metal units and decreases by collisions of the particles composed of k units with the other particles. Consequently, for a homogeneous surface,

$$\frac{dN_{v_k}}{dt} = \frac{1}{2}\sum_{i+j=k} K_{ij}N_{v_i}N_{v_j} - N_{v_k}\sum_{i=1}^{\infty} K_{ik}N_{v_i} \tag{2}$$

where K_{ij} are second-order rate constants dependent upon the mobility of the particles on the support and on the nature of the interaction between the particles (*9*).

For the two limiting situations of "diffusion control" and "sintering control" the rate constants K_{ij} are given by (*9*)

$$K_{ij} = \frac{8D_{ij}}{\pi}\int_0^{\infty} e^{-D_{ij}u^2\theta'} \times \frac{du}{[J_0^2(uR_{ij}) + Y_0^2(uR_{ij})]u} \qquad \text{(diffusion control)} \tag{3}$$

and

$$K_{ij} = 2\pi R_{ij}\alpha_{ij} \qquad \text{(sintering control)}. \tag{4}$$

α_{ij} is a reaction-rate constant for the merging process, $R_{ij} = R_i + R_j$ is the radius of interaction of the two colliding particles, and D_{ij} is the diffusion coefficient of particle i with respect to particle j.

As pointed out previously (*9*), the present approach involves two time scales: a large scale of time t, introduced in Eq. (2), which coincides with the time of the process, and a small scale of time θ', used in the calculation of the rate of collisions and thus of the rate constants K_{ij}. In the case of sintering control, the rate constants are independent of the small-scale time [Eq. (4)], because the small time affects only the rate of diffusion of the particles towards a selected particle. In this situation the diffusion is not the rate-determining step. In the case of "diffusion control," the rate constants depend on the small-scale time, but in certain situations this dependence is after a very short time very weak (see Appendix I) and

$$K_{ij} = \frac{4\pi D_{ij}}{\ln 4T}, \tag{3'''}$$

(where $T = D_{ij}\theta'/R_{ij}^2$) becomes a good approximation for Eq. (3). Equation (2) together with Eqs. (3''' and 4) describes the sintering process in the two limiting situations. These equations will be used to obtain both the time dependence of the particle-size spectrum and the time evolution of the exposed surface area.

The surface of the support is in reality nonhomogeneous from a topographic and energetic point of view. Some sites can interact so strongly with the crystallites that they are immobilized; also some regions of the surface can entrap crystallites.

Besides the quantities N_{v_k} representing the number of moving crystallites per unit

surface area of support, the quantities F_{v_k} representing the number of fixed crystallites per unit surface area of support composed of k metal units are now of significance. Two probabilities are introduced. The probability p that a particle formed by the collision of two moving particles will form a mobile particle and the probability q that a trapped particle will become mobile after a collision with a moving particle. The probability p is a consequence of the fact that some of the collisions take place, either over sites which can interact strongly with the crystallites, or over trapping regions. For simplicity sake p and q are assumed size independent. The moving particles can encounter trapping regions becoming fixed. This is equivalent to introduce in the equations a first-order chemical reaction of the type $\beta_k N_{v_k}$.

The concentration N_{v_k} increases by the collisions between moving particles composed of i and $k - i$ metal units which lead to mobile particles, and by the collisions between moving particles of i units and fixed particles of $k - i$ units which generate moving particles. It decreases by trapping and by collisions between the moving particles of k units and all the other particles.

The concentration F_{v_k} increases by trapping of mobile particles, by the collisions between moving particles of i metal units and fixed particles of $k - i$ units which generate immobilized particles, and by the collisions between moving particles of i and $k - i$ units which form fixed particles. It decreases by collisions between fixed particles of k units and all the moving particles.

Therefore, the rate of change of N_{v_k} and F_{v_k} can be written as

$$\frac{dN_{v_k}}{dt} = \frac{1}{2} p \sum_{i+j=k} K_{ij} N_{v_i} N_{v_j} - N_{v_k} \sum_{i=1}^{\infty} K_{ik} N_{v_i} - N_{v_k} \sum_{i=1}^{\infty} K^*_{ki} F_{v_i} + q \sum_{i+j=k} K^*_{ij} N_{v_i} F_{v_j} - \beta_k N_{v_k} \quad (5a)$$

and

$$\frac{dF_{v_k}}{dt} = (1 - q) \sum_{i+j=k} K^*_{ij} N_{v_i} F_{v_j} + \frac{1}{2} (1 - p) \sum_{i+j=k} K_{ij} N_{v_i} N_{v_j} - F_{v_k} \sum_{i=1}^{\infty} K^*_{ik} N_{v_i} + \beta_k N_{v_k} \quad (5b)$$

Equations for the rate constants K^*_{ij} can be obtained as in our previous paper (*9*) taking however into account the trapping and replacing the diffusion coefficient D_{ij} of particle i with respect to particle j ($D_{ij} = D_i + D_j$) by the diffusion coefficient D_i of the moving particle. The rate constants K_{ij} must also be recalculated.

Effect of the Rate Determining Step of the Sintering Process on the Particle Size Distribution for Homogeneous Surfaces

The equations for the discrete spectrum of particle sizes were solved numerically for the initially unisized distribution: $N_{v_{i,0}} = N_0$ for $i = 1$ and $N_{v_{i,0}} = 0$ for $i \neq 1$. A fourth-order Runge–Kutta method was used and as many equations (up to 800) considered as were needed to ensure that no particle was lost in the calculations. Errors due to the underflow of the computing machine were negligible.

The two limiting cases of "sintering control" [Eqs. (2 and 4)] and "diffusion control" [Eqs. (2 and 3‴)] are considered for various size dependencies of the diffusion coefficients and reaction rate constants (see Table 1).

In Figs. 1 to 5 are plotted the results obtained for the size distribution at different times and for different mechanisms. For "diffusion control" (Figs. 1–3) the particle-size distributions develop a maximum because the rate constants K_{ij} decrease with increasing particle size, and therefore the smallest particles in the system disappear the fastest (see also Fig. 6). For "sintering control" a monotone decreasing particle size distribution is obtained (Figs. 4 and

TABLE 1

TIME EVOLUTION OF EXPOSED METAL SURFACE AREA IN THE TWO LIMITING CASES (9)

Diffusion control Assumed size dependence of D_{ij}	Rate constants	Rate equation for exposed surface area
$D_{ij} = C_1\left(\frac{1}{r_i^2} + \frac{1}{r_j^2}\right)$	$K_{ij} = C'_1\left(\frac{1}{r_i^2} + \frac{1}{r_j^2}\right)$	$\frac{dS}{dt} = -C''_1 S^6$ (I-1′)
$D_{ij} = C_2\left(\frac{1}{r_i} + \frac{1}{r_j}\right)$	$K_{ij} = C'_2\left(\frac{1}{r_i} + \frac{1}{r_j}\right)$	$\frac{dS}{dt} = -C''_2 S^5$ (I-2′)
$D_{ij} = C_3$	$K_{ij} = C'_3$	$\frac{dS}{dt} = -C''_3 S^4$ (I-3′)
Kinetic control Assumed size dependence of α_{ij}	Rate constants	Rate equation for exposed surface area
$\alpha_{ij} = C_4$	$K_{ij} = C'_4(r_i + r_j)$	$\frac{dS}{dt} = -C''_4 S^3$ (I-4′)
$\alpha_{ij} = C_5 \frac{r_i^2 + r_j^2}{r_i + r_j}$	$K_{ij} = C'_5(r_i^2 + r_j^2)$	$\frac{dS}{dt} = -C''_5 S^2$ (I-5′)

5) because the rate constants K_{ij} increase with increasing particle size, and therefore the smallest particles in the system disappear most slowly (Fig. 7).

In Fig. 8 the results obtained for the size distributions for the same value of the ratio S_0/S and for different mechanisms are compared. The particle-size distributions for the diffusion-controlled cases are significantly narrower than those obtained for

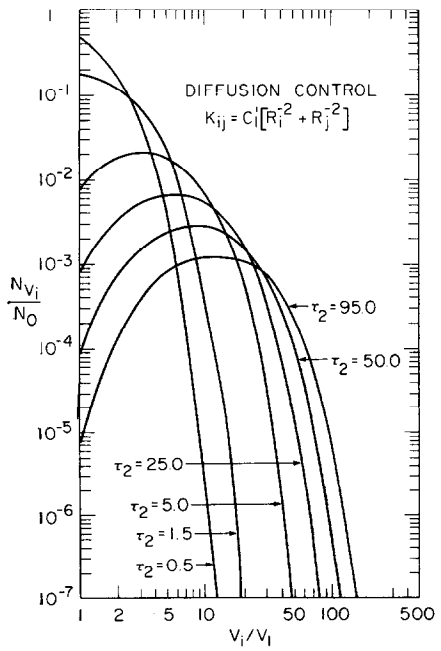

FIG. 1. Particle size distribution from numerical solution of kinetic equations; unisized initial distribution.

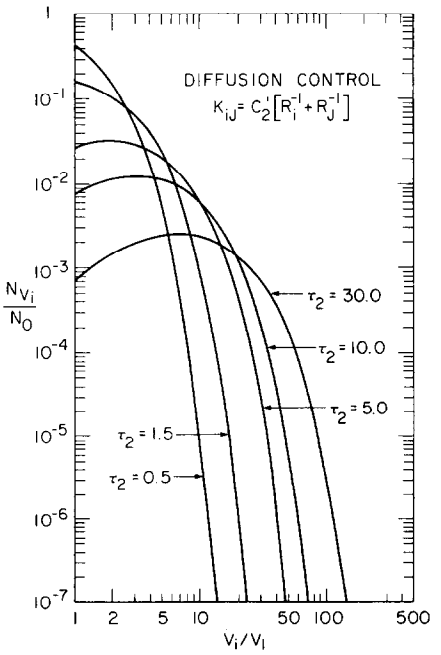

FIG. 2. Particle size distribution from numerical solution of kinetic equations; unisized initial distribution.

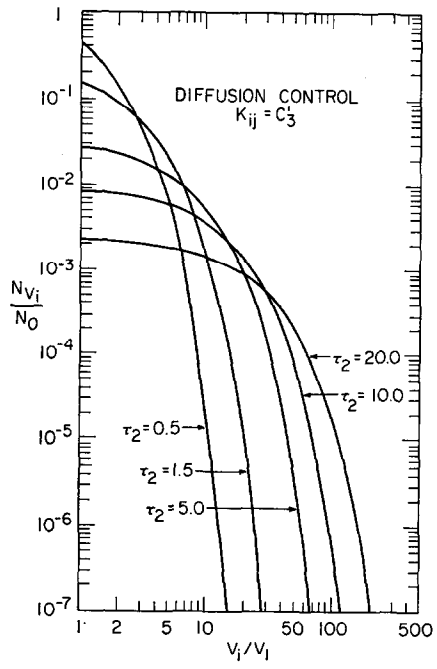

FIG. 3. Particle size distribution from numerical solution of kinetic equations; unisized initial distribution.

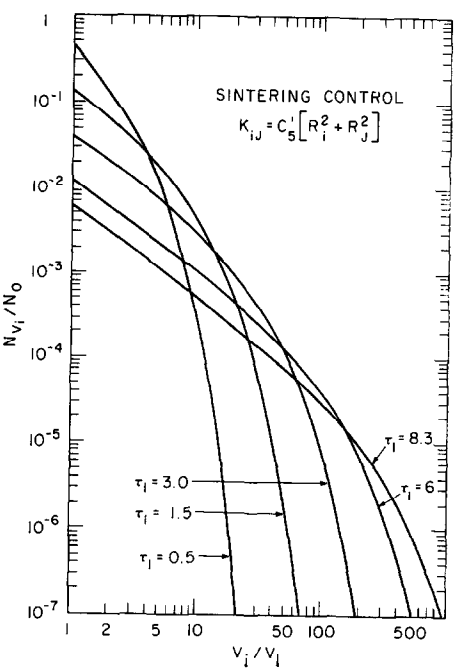

FIG. 5. Particle size distribution from numerical solution of kinetic equations; unisized initial distribution.

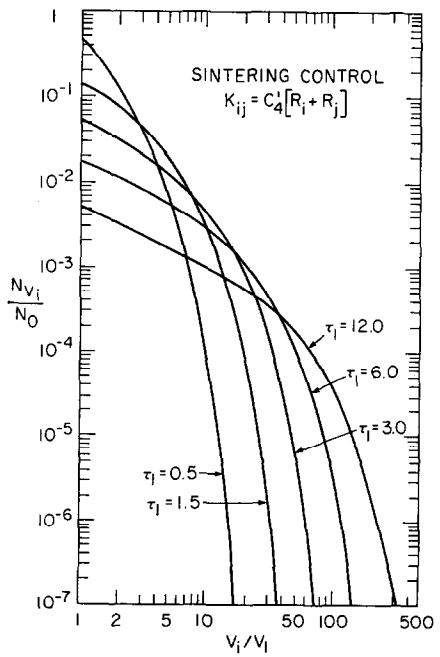

FIG. 4. Particle size distribution from numerical solution of kinetic equations; unisized initial distribution.

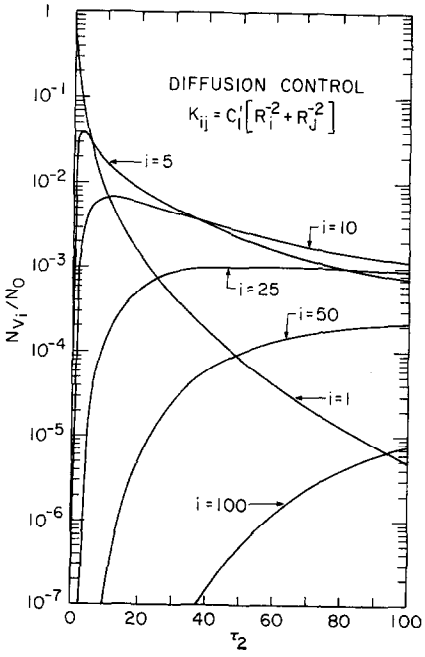

FIG. 6. Number of particles of volume v_i as a function of the dimensionless time τ_2; unisized initial distribution.

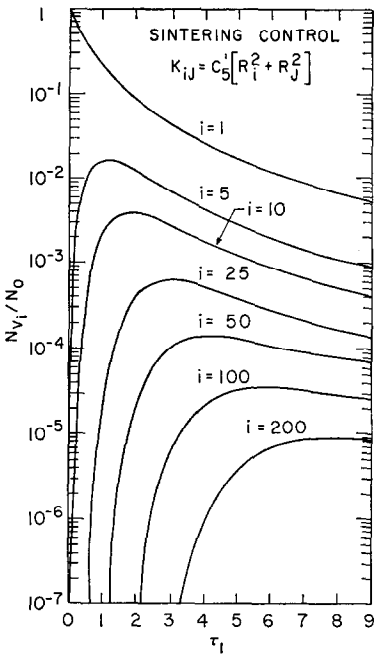

FIG. 7. Number of particles of volume v_i as a function of the dimensionless time τ_1; unisized initial distribution.

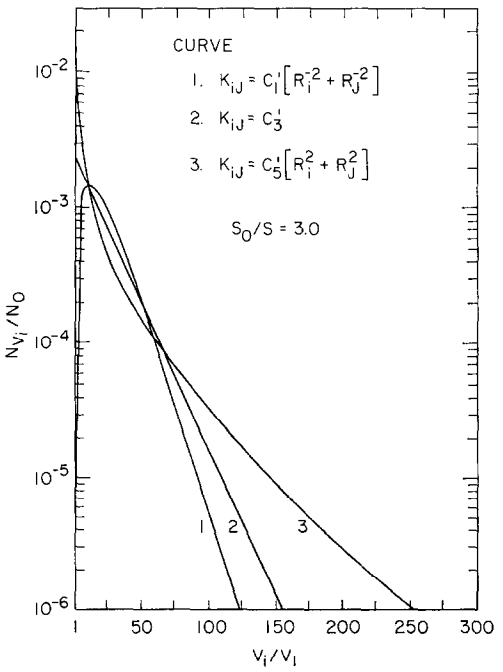

FIG. 8. Particle size distribution for "diffusion control" and "sintering control" for the ratio $S_0/S = 3$, unisized initial distribution.

the sintering-controlled cases. This result suggests a criterion to differentiate between the two mechanisms.

For initial size distributions different from the unisized, our calculations show that for sufficiently long times the size distributions are very similar, approaching the curves obtained for an initially unisized distribution. This result raises the question of the possibility of superposing on a unique curve the time-dependent size spectra. It is shown in Appendix II that such a unique spectrum is obtained if the dimensionless groups $N_{v_i}\phi/v_1N^2$ and v_iN/ϕ are used as variables, where N is the total number of particles per unit surface area of support at a given time t, and ϕ is the total volume of metal per unit surface area. Such a unique spectrum was first used in a different context (size distribution of aerosols) by Friedlander (*34*, *35*).

In Fig. 9 the size distributions for the diffusion-controlled case are plotted using these dimensionless groups. Two different initial distributions are considered. For both, the initially monodispersed and exponentially dispersed spectrum, the unique

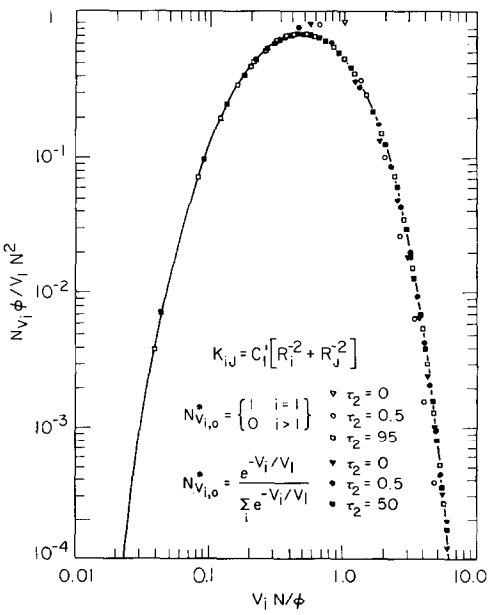

FIG. 9. Dimensionless size distribution for "diffusion control" and different initial distributions; the solid curve represents the similarity solution.

spectrum (solid line) is reached within a short time ($\tau_2 \simeq 2.5$).

Time Evolution of Exposed Surface Area for Homogeneous Surfaces

It will be assumed that the general shape of the particles is preserved during the growth process. Consequently the exposed surface area of a particle containing k units is given by

$$S_k = S_1 k^{2/3}, \tag{6}$$

where S_1 is the exposed surface area of a particle containing one unit. The time evolution of the rate of change of the exposed surface area may be calculated from

$$\frac{dS}{dt} = S_1 \sum_{k=1}^{\infty} k^{2/3} \frac{dN_{v_k}}{dt}. \tag{7}$$

In our previous paper (*9*) the equations for the decay of the surface area [Eqs. (2 and 7)] were solved numerically for an initially unisized distribution. The two limiting cases of "sintering control" and "diffusion control" were considered, taking various size dependencies of the diffusion coefficients and the reaction rate constants into account. The results obtained are summarized in Table 1.

One may observe that the rate equation of the exposed surface area is very sensitive to the rate determining step of the process. In the case of "sintering control" exponents of 3 and smaller are obtained for n [Eq. (1)] while for "diffusion control" the exponent is 4 or larger.

These results, obtained previously for an initially unisized distribution, are of more general validity, because, as shown here, after a relatively short time the size distribution can be represented by the similarity variables. In Appendix II an equation for the decay of the exposed surface area of the metal is derived on the basis of the similarity variables. The resulting equation [Eq. (19) from Appendix II] is indeed equivalent to those established on the basis of numerical computations for an initially unisized distribution (Table 1). The exponent of S in the rate equation for the decay of the exposed surface area of metal [Eq. (1)] is thus dependent only on the assumed mechanism of the process and on the size dependence of the diffusion coefficient and reaction-rate constants, and it is almost independent of the initial distribution.

Size Distribution and Exposed Surface Area for Nonhomogeneous Surfaces with Some Sites which Interact Strongly with Crystallites

In this case, an equilibrium size distribution is reached. Because the strong interacting sites have been active during the preparation process favoring the formation of crystallites, one may expect that a large fraction of these sites are covered by the immobile crystallites from the beginning. Neglecting the trapping regions, one may assume that $p = 1$ and $\beta_k = 0$. Figure 10 shows the size distribution, close to equilibrium, obtained for different values of the initial ratio between moving and fixed islands and for an initially unisized size distribution. By "close to equilibrium" we understand here that less than 1/10 of the particles present are still mobile. Figures 11–13 show the time evolution of the size distribution of the moving particles, fixed

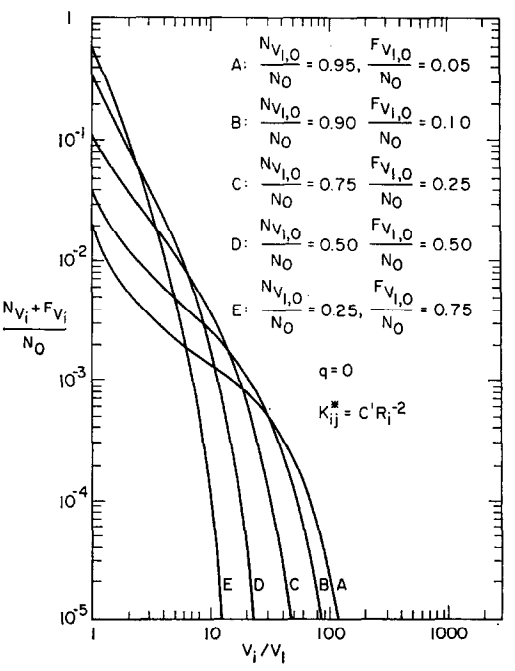

FIG. 10. Particle size distribution in the nonhomogeneous case, close to equilibrium.

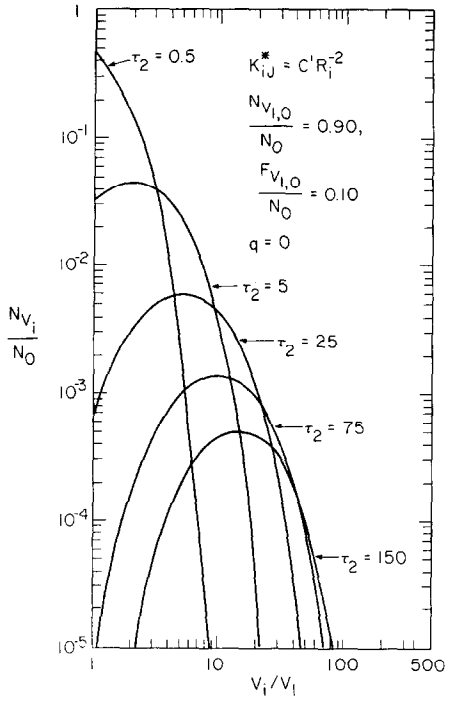

FIG. 11. Time dependence of the size distribution of the moving particles, in the nonhomogeneous case.

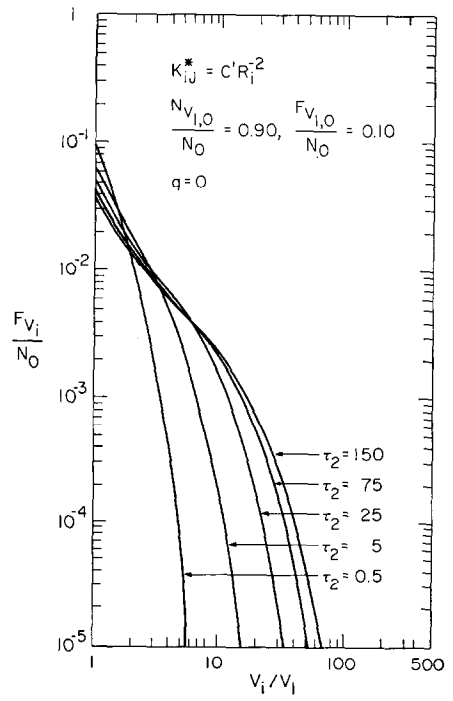

FIG. 12. Time dependence of the size distribution of the fixed particles, in the nonhomogeneous case.

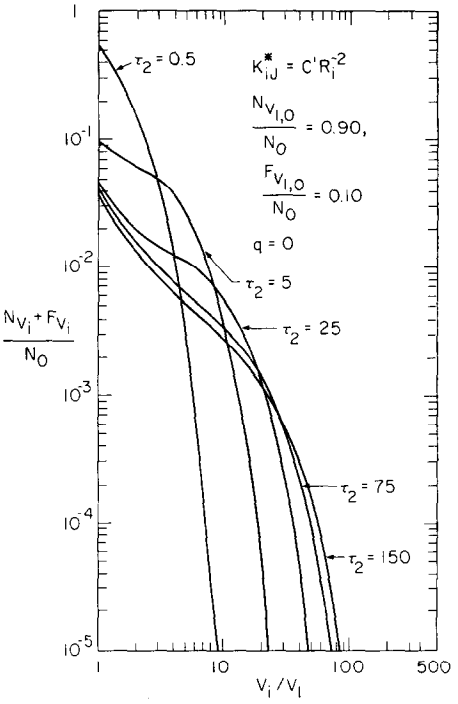

FIG. 13. Time dependence of the size distribution of the total number of particles, in the nonhomogeneous case.

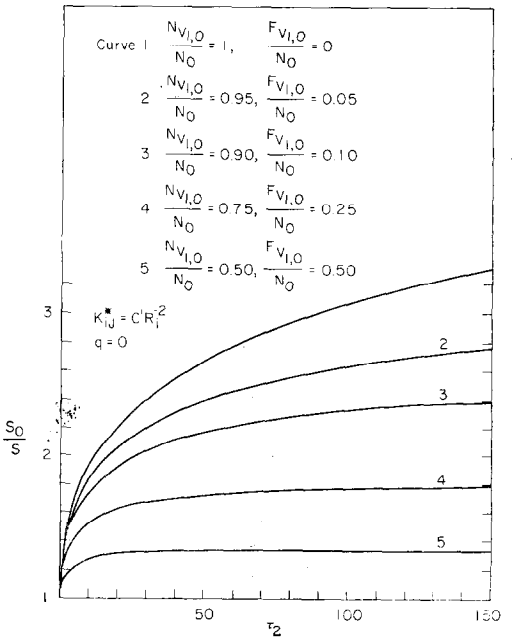

FIG. 14. Effect of fixed islands on the time dependence of S_0/S.

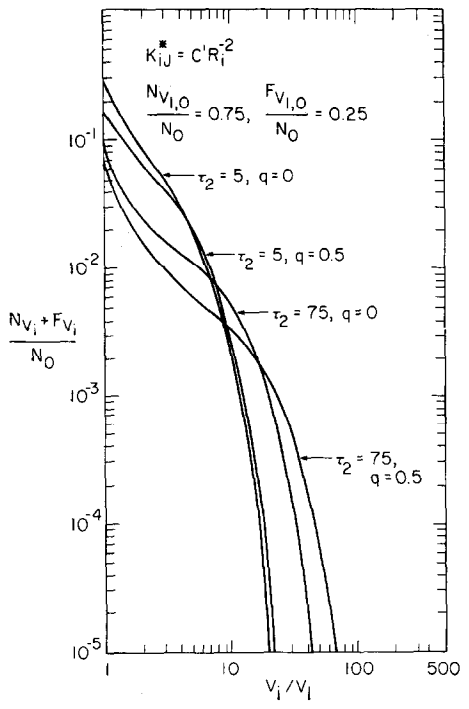

FIG. 15. Effect of the probability q on the time dependence of the size distribution of the total number of particles.

particles, and total number of particles for a specific example. Figure 14 shows the effect of fixed islands on S_0/S for $q = 0$ and various initial values of the ratio N_{v_1}/F_{v_1}. Figure 15 shows the effect of the probability q on the distribution of sizes.

The main conclusions are: (a) a narrow equilibrium size distribution is reached from an initially unisized distribution even if the ratio between mobile and fixed particles is initially as large as 20; (b) the equilibrium size distribution is strongly dependent on the initial distribution (as opposed to the similarity solution obtained previously); (c) an equilibrium value is reached for S; and (d) the size distribution is somewhat broadened when $q = 0.5$. Because small values of q are expected, its influence appears to be of secondary importance.

DISCUSSION AND COMPARISON OF MODEL PREDICTIONS WITH EXPERIMENTAL RESULTS

Table 2 is a list of the experimental data available for the exposed metal surface area of Pt-on-alumina catalysts during heat treatment. One may observe that the exponent in the decay equation of the exposed surface area of metal is in the range 2–8, thus covering both the cases of "sintering control" and "diffusion control."

The results obtained in the particular cases can be interpreted as follows: Maat and Moscou (*1*) measured the rate of sintering of a platinum reforming catalyst at a temperature of 1053 K (Table 2, row 1), probably in an oxidizing atmosphere. They found that the decay of the exposed platinum area followed second order kinetics, which, according to the present considerations, shows a sintering controlled decay. By means of electron microscopy they determined a large dispersion of the particle size distribution. The initial size distribution was between 10 and 50 Å, with an average particle size close to 10 Å. After 17 hr of sintering the distribution was between 10 and 500 Å. Both the observation of a large dispersion of the particle sizes after sintering and the observation that the smallest particles existing initially were still present after excessive sintering (~15-fold decrease in surface area after 17 hr of sintering) are in qualitative agreement with a sintering controlled mechanism.

Herrmann *et al.* (*6*) reported data on the sintering kinetics of Pt–Al_2O_3(Cl) and Pt–Al_2O_3(F, Cl) reforming catalysts in the temperature range 837–898 K (Table 2, row 2) and a dry air atmosphere. The exposed surface area of metal was measured by hydrogen chemisorption. They found that the rate of decrease of the metal surface area—especially at 898 K—was second-order with respect to the metal surface area, thus indicating a sintering-controlled decay.

Gruber (3) reported data on the sintering behavior of Pt-on-alumina catalyst prepared by tetrammino platinum hydroxide impregnation. The sintering experiment was carried out at 773 K (Table 2, row 3) in a reducing atmosphere. Their data can be represented by a sixth-order reaction, which according to the present considerations, is an indication of diffusion controlled decay.

TABLE 2

TIME EVOLUTION OF EXPOSED SURFACE AREA; EXPERIMENTAL RESULTS AND THEIR INTERPRETATION

		Experimental results			Model interpretation	
	Reference	Type of catalyst	Temperature and atmosphere	Rate of decay of exposed metal surface	Controlling	Diffusion coefficient or reaction rate constant
1	(*1*)	Pt on γ-Alumina 0.5–0.7% Cloride 0.6% Pt 140–180 m^2/g support	1053 K Probably dry air	$\frac{dS}{dt} = -K_1S^2$	Sintering	$\alpha_{11} = 4. \times 10^{-9}$ cm/sec based on particle 10 Å in size
2	(*6*)	Pt on γ-Alumina a) 0.83% Cl, 0.774% Pt 225 m^2/g support b) 0.35% Cl, 0.35% F 0.375% Pt 176 m^2/g support	898 K Dry air	$\frac{dS}{dt} = -K_2S^2$	Sintering	$\alpha_{11} = 1. \times 10^{-9}$ cm/sec based on particle 10 Å in size
3	(*3*)	Pt on γ-Alumine 1.1% Pt 210 m^2/g support	773 K H_2	$\frac{dS}{dt} = -K_3S^6$	Diffusion	$D_1 \simeq 8. \times 10^{-18}$ cm^2/sec based on particle 10 Å in size
4	(*7*)	Pt on Alumina	755 K 811 K H_2	$\frac{dS}{dt} \simeq -K_4S^8$ $\frac{dS}{dt} \simeq -K_5S^{7.8}$	Diffusion	

Hughes *et al.* (*7*) (Table 2, row 4) obtained results similar to those of Gruber (*3*). They measured the exposed surface area of metal as a function of time at 755 and 811 K in a reducing atmosphere. The experimental rate of decay of the exposed surface area of metal indicates a diffusion mechanism, however, with a stronger size-dependent diffusion coefficient than in Gruber's experiments.

We stress that even a qualitative discussion of the above-mentioned data leads to the conclusion that two different mechanisms occur. In some of the cases the decay of the exposed metal surface area is rapid, being for instance a 15-fold decay after 17 hr of heating in an oxidizing atmosphere at 1053 K (*1*) and a 12.5-fold decay after 40 hr at 898 K (*6*). As opposed to these situations, Gruber (*3*) reports that at 773 K and in a reducing atmosphere a heat treatment of 1200 hr leads to only a 2.5-fold decay of the exposed surface area of metal, while Hughes *et al.* (*7*) observed a 3-fold decay after 1000 hr at 811 K also in a reducing atmosphere. Consequently, a decrease in temperature from 1053 to 898 K and in an oxidizing atmosphere results in a decrease of the rate of sintering by about a factor of 4. A further drop in temperature by another 100 K together with a change of the chemical atmosphere to a reducing atmosphere slows down the sintering by more than two orders of magnitude, and changes the exponent n in the rate equation [Eq. (1)] substantially. Obviously the decay of the surface area of metal is controlled in those situations by different processes.

As suggested by the present treatment, the rate of the process is either controlled by the random motion of the crystallites on the surface of the support or by the merging of two colliding particles into a single

particle. At sufficiently high temperatures the mobility of the crystallites upon the support is high and one may expect that the merging process is the rate-determining step. For not too high temperatures, the mobility of the crystallites is lower and consequently the diffusion of the crystallites on the support prevails. The data presented above are compatible with this explanation showing that at high temperatures the process is indeed controlled by the merging process, while at lower temperatures the process is diffusion controlled.

The rate of decay depends also on the chemical atmosphere (*5, 7, 8, 17*). At the same temperature the rate of decay is much higher in an oxidizing than in a reducing atmosphere (*5, 17*). Our theoretical approach can explain such behavior, because the diffusion coefficients of the crystallites and the reaction-rate constants of the merging process depend upon the surface properties of the system. The chemisorption process essentially changes the surface free energies and the surface diffusion of the metal on the metal. If the wetting angle of the crystallite on the support becomes larger, due to the changes in the surface free energies, then the surface of crystallite–support contact becomes smaller and consequently their interaction smaller.† In this case the mobility (diffusion coefficient) of the crystallite is increased. The merging process also depends upon the surface free energy and surface diffusion of the metal atoms on the metal surface (*18*). For instance, the surface diffusion coefficient of copper atoms on copper is increased by a factor of about 5 in the presence of oxygen compared to a reducing atmosphere (*19*).

No data are yet available to establish the effect of chemical atmosphere on the wetting angles between metals and supports used in supported metal catalysts. Some data, however, for the wetting angle of drops of $Na_2Si_2O_5$-glass on several metals show an important effect of the atmosphere on the wetting angle (*20, 21*).

Some authors have suggested that a possible explanation for the increase in the rate of sintering in an oxygen atmosphere is the mass transfer caused by formation and vaporization of PtO_2 (*5, 17*). Information available in the literature concerning platinum wires or bands shows that the losses of platinum in an oxygen atmosphere are negligible at temperature below 1050 K (*22–24*). Though for the small crystallites of interest here the vapor pressure is increased due to the curvature effect, our evaluations show that the rate of vaporization [limited in the present case by the diffusion of PtO_2 molecules away from the surface (*25*)] for the temperature range of interest remains negligibly small.

The diffusion coefficient computed by us are very small, of the order of 10^{-17} cm^2/sec at 773 K for a crystallite 10 Å in diameter (Table 2). The values measured for the diffusion coefficient of aluminum islands of the same size on KCl at even lower temperatures are larger by several orders of magnitude, 10^{-12}–10^{-14} cm^2/sec (*26, 27*). The reason for this difference probably lies in the nature of the interactions between metal and support, interactions which depend upon the roughness of the surface of the support and the nature of the bonds between the metal and support. Obviously in the cases in which the pores are not sufficiently large compared to the size of the crystallites, another restriction appears.

Concerning the interactions between metal and support, let us observe that for small aluminum islands evaporated onto the KCl-substrate and also for metal crystallites of a completely reduced supported metal catalyst, relatively weak interactions of the van der Waals type are dominant (*18*). The preparation history of the supported catalyst, on the other hand (for example preparation by adsorption (or ion exchange) as opposed to preparation by impregnation) might influence the nature of the bonds at the metal–substrate interface: If the catalyst is prepared by adsorption from a solution containing for

† For very small crystallites the surface free energies and the wetting angle depend upon their dimensions. Our discussions imply the assumption that their qualitative behavior is as for large objects.

example $(Pt(NH_3)_4)Cl_2$, then during preparation strong ionic bonds are formed between the acidic groups of the support and $Pt(NH_3)_4^{2+}$ (*4*). In the impregnation procedure no such strong interaction between the platinum salt and the support exists. Perhaps even after reduction the strong ionic metal–substrate bonds are partly preserved in the catalyst prepared by adsorption, thus leading to decreased mobility of the particles. Consequently, a higher stability of the highly dispersed state of metal is expected if the support is more acidic and an adsorption procedure is used for the preparation of the supported metal catalyst.

During preparation of the supported metal catalyst, high temperatures are often used, in particular in the reduction period. Thus migration and sintering of the unreduced platinum can also occur. The extent of sintering depends on the temperature, on the duration of the reduction period, and as discussed above, on the method of preparation. Consequently a higher degree of sintering is expected during the reduction period for an acidic support when the impregnation rather than an adsorption method is used. There is experimental confirmation (*4, 29*) of this observation.

It was shown above that for diffusion control the particle-size distribution can be represented by a unique spectrum after a dimensionless time $\tau \simeq 2.5$. (For the catalyst used by Maat and Moscou and for a diffusion coefficient of about 10^{-14} cm^2/sec, one obtains a time of the order of 500 sec.) It is natural to expect that the size distribution for a freshly prepared catalyst, when reduced at high temperatures, can be represented by the unique spectrum. In Fig. 16, the experimental results of Wilson and Hall (*28, 29*) are compared with the theoretical predictions. The ratio

$$\sum_{i}^{\infty} N_{v_k} \Big/ \sum_{1}^{\infty} N_{v_k}$$

rather than ψ^* is selected as a variable both because it is convenient and because, like ψ^* it is dependent only on η_i^*. Theory and experiment are in good agreement in showing that the size distribution of

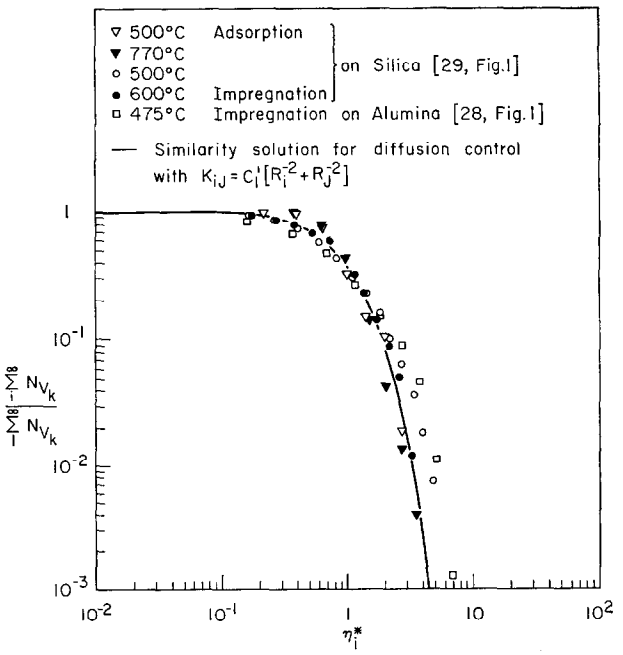

FIG. 16. Comparison between the theoretical similarity solution and Wilson and Hall experimental data for size distribution in fresh catalyst prepared at high reduction temperature.

freshly prepared catalysts reduced at high temperatures already follows the unique spectrum closely.

There are some data in the literature (*2*) which appear to show that after a sufficiently long time of heat treatment sintering no longer occurs. Probably that in those cases the surface was nonhomogeneous and the equilibrium distribution was reached.

Possible Improvements of the Stability of a Highly Dispersed State of Metal

From the previous discussion it results that the stability of a highly dispersed state of metal may be increased by controlling (a) the wetting angle of the metal crystallites, (b) the interactions between the metal and support, (c) the merging behavior of two colliding particles into one particle, (d) the number of fixed islands.

(a) The wetting angle can be changed if, instead of using a pure metal, surface active metals are also present as impurities. Some information concerning the variation of the wetting angle with the concentration c of a soluble impurity can be obtained from Young's equation

$$\sigma_{sg} - \sigma_{ss'} = \sigma_{s'g} \cos\theta \tag{8}$$

Taking the derivative with respect to c, one obtains

$$\frac{d\sigma_{sg}}{dc} - \frac{d\sigma_{ss'}}{dc} = \cos\theta \frac{d\sigma_{s'g}}{dc} - \sin\theta\, \sigma_{s'g} \frac{d\theta}{dc} \tag{9}$$

Gibbs' equation allows us to write

$$\frac{d\sigma_{sg}}{d\mu} = -\Gamma_{sg}; \quad \frac{d\sigma_{ss'}}{d\mu} = -\Gamma_{ss'}; \quad \frac{d\sigma_{s'g}}{d\mu} = -\Gamma_{s'g} \tag{10}$$

where Γ_{sg} is the surface excess concentration of the impurity on the support–gas interface, $\Gamma_{ss'}$ is the surface excess concentration of the impurity on the support–metal interface, $\Gamma_{s'g}$ is the surface excess concentration on the metal–gas interface, and μ is the chemical potential. For simplicity it is assumed that the solid solution is ideal. Consequently,

$$d\mu = RT d\ln c \tag{11}$$

Equation (9) becomes

$$\sigma_{s'g} \sin\theta \frac{d\theta}{d\ln c} = RT(\Gamma_{sg} - \Gamma_{ss'} - \cos\theta\Gamma_{s'g}). \tag{12}$$

In the situations in which $\Gamma_{sg} - \Gamma_{ss'} - \cos\theta\Gamma_{s'g} < 0$, the impurity contributes to the decrease of the wetting angle and consequently to a lower mobility of the crystallites. If no adsorption occurs on the support–gas interface near the leading edge of the crystallite, then a decrease in the wetting angle will always take place when the surface active metal is preferentially adsorbed on the solid–solid interface.

(b) If the impurity is soluble in the support, then the mobility of the crystallite will decrease because a stronger interaction between the crystallite and support is induced. In terms of concepts from surface chemistry, the stronger interaction has as a consequence the decrease of the surface tension solid–solid and consequently of the wetting angle. Indeed, the surface tension solid–solid, $\sigma_{ss'}$, is related to the surface tensions σ_{sg} and $\sigma_{s'g}$ by the equation**

$$\sigma_{ss'} = \sigma_{sg} + \sigma_{s'g} - U_{ss'} + U_{str'} \tag{13}$$

where $U_{ss'}$ is the interaction energy per unit surface area between the atoms on one side of the interface and the atoms on the other side of the interface, and U_{str} is the strain plus the dislocation or fracture energies per unit surface area, induced by the disregistry between the lattices of the support and of the metal. Consequently $\sigma_{ss'}$ decreases when $U_{ss'}$ increases. Equation (13) can be understood if one considers the limiting situation of two parts of the same solid body separated by an imaginary plane. In this case $\sigma_{ss'}$ must be zero.

However, too much impurity dissolved in the support may have a destructive effect upon the support structure, increasing much more the term U_{str} than the term $U_{ss'}$. In this situation the surface

** The quantity $W = \sigma_{sg} + \sigma_{s'g} - \sigma_{ss'} = U_{ss'} - U_{str}$ represents the work of adhesion.

tension $\sigma_{ss'}$ is increased and consequently (assuming that the other two surface tensions are not affected much) the wetting angle and the mobility of the crystallite increase. One thus may expect that the mobility will be decreased for small concentration of the impurity and increased for large concentrations. Of course the surface active impurities also influence the values of $\sigma_{s'g}$ and σ_{sg}.

There are some experimental results in the literature (*30*) concerning the effect of interfacially active metals on the wetting and adhesion of liquid nickel drops to α-Al_2O_3. They can be interpreted on the basis of the above considerations. For high-purity nickel at 1773 K and 5×10^{-6} Torr the contact angle $\theta = 100.7$ degrees, the surface tension at the Ni–Al_2O_3 interface is equal to 1290 ergs/cm^2 and the work of adhesion to 1390 ergs/cm^2. Addition of 0.99 atomic% titanium to the nickel resulted in a decrease of the wetting angle to 94.5 degrees, a decrease of the surface tension at the Ni–Al_2O_3 interface to 1090 ergs/cm^2 and an increase of the work of adhesion to 1640 ergs/cm^2. Using electron beam X-ray microanalysis, it was found that the titanium was concentrated in the vicinity of the nickel–support interface, resulting in an increase of the adhesion of the drop to the support.

Addition of 1 atomic% zirconium to the high purity nickel resulted in an increase of the wetting angle to 136.2 degrees; in an increase of the surface tension at the Ni–Al_2O_3 interface to 2220 ergs/cm^2; and in a decrease of the work of adhesion to 500 ergs/cm^2. Electron photomicrographs revealed that the zirconium was concentrated in the vicinity of the nickel–substrate interface, chemically reducing the Al_2O_3 support and weakening its structure. The energy U_{str} was thus increased, resulting in a decreased adhesion of the drop to the support. One may conclude that the stability of the highly dispersed state of metal on a support may be substantially increased if certain alloys are used rather than pure metals. The higher stability of reforming catalysts obtained by Sinfelt (*31*) and his group can probably be explained on the basis of the above considerations.

(c) The rate of sintering of two spheres in contact increases with increasing surface diffusion and surface tension (*32*). The sintering of two spherical caps of different radii on a support has not yet been studied from a theoretical point of view. In the last case the surface tension at the metal–support interface will also play a role and the rate of sintering will be decreased with increasing metal–support interactions.

(d) As shown in Section 4 the stability of the catalyst can be much improved if some strongly interacting sites can be generated. Perhaps this can be done using a double adsorption or double impregnation procedure in which first a small amount of metal which interacts strongly both with the active metal and support is introduced.

Regeneration of Catalyst

Regeneration by heating in an oxygen atmosphere of the catalyst containing sintered crystallites (*3, 36, 37, 38*) can be also explained in terms of wetting. Indeed, the new chemical atmosphere can modify the surface free energies in such a manner that the spreading coefficient χ becomes larger than zero

$$\chi \equiv \sigma_{sg} - \sigma_{ss'} - \sigma_{s'g} > 0. \qquad (14)$$

For a crystallite in equilibrium

$$\frac{\sigma_{sg} - \sigma_{ss'}}{\sigma_{s'g}} = \cos\theta \leq 1 \qquad (15)$$

A spreading coefficient larger than zero is not compatible, however, with $\cos\theta \leq 1$. Consequently if $\chi > 0$ the initial crystallite will no longer be stable, but will split and redisperse. The kinetics of splitting will be analyzed in a subsequent paper.

Conclusion

The aging kinetics of supported metal catalysts are determined by the diffusion of the crystallites upon the surface of the support and by the rate of sintering of the colliding crystallites. The equations obtained on the basis of this model describe the time dependence of the size distribu-

tion and the decay of the exposed surface area of metal.

The theory can explain (a) the influence of the preparation procedure, (b) the influence of the atmosphere, and (c) the influence of the temperature upon the rate of decay of the exposed surface area of the metal.

Considerations based upon the wetting (adhesion properties) of the metal on the support suggest possibilities for improving the stability of the highly dispersed state of the metal on the surface of the support.

Appendix I. Time Dependence of the Rate Constants in the Diffusion Model

In the case of diffusion control the present approach involves two time scales, a long time scale t, introduced in Eq. (2), which coincides with the time of the process, and a small time scale θ', used in the calculation of the rate constants K_{ij}. The present treatment can be used if the rate constants are only weakly time-dependent after a time which is sufficiently short compared to the time of the process (*9*). Values for the small scale time are not provided by the theory, but it is reasonable to assume that they are of the order of the time needed for sufficiently small variations of the concentrations N_{v_i} to occur.

Equation (3), valid for "diffusion control," can be approximated by:

$$K_{ij} = 2D_{ij}\pi \left[(\pi T)^{-1/2} + \frac{1}{2} - \frac{1}{4}(T/\pi)^{1/2} + \frac{1}{8} T \cdots \right], \quad (3')$$

for small values of $T = D_{ij}\theta'/R_{ij}^2$, and by

$$K_{ij} = 4D_{ij}\pi \left[\frac{1}{\ln (4T) - 2\gamma} - \frac{\gamma}{[\ln (4T) - 2\gamma]^2} \right] \cdots, \quad (3'')$$

for large values of T. Here $\gamma = 0.5772$ is Euler's constant. If $\ln 4T \gg 2\gamma \simeq 1$, then Eq. (3'') may be further simplified to give

$$K_{ij} = \frac{4\pi D_{ij}}{\ln T4}. \quad (3''')$$

Let us first assume that D_{ij} is of the order of a surface diffusion coefficient, 10^{-4} to 10^{-10} cm^2/sec (*33*). The collision radius R_{ij} is of the order of the particle sizes present in the system (10^{-6} to 10^{-7} cm). Consequently, the dimensionless time T is of the order of (10^2 to 10^{10}) $\times \theta'$ and hence is long after a very short time θ'. Since for such large values of T the strong inequality $\ln 4T \gg 1$ is satisfied, Eq. (3') can be approximated by Eq. (3'''). Although the rate constants depend on the small scale time, this time-dependence is after a short time very weak (Fig. 17). Consequently, K_{ij} from (3''') can be considered constant and the present treatment in which no possibility for determining θ' exists can be used.

The mobility of the crystallites on the support is, however, much smaller than that of the molecules due both to their larger sizes and to stronger metal–support interactions. For this reason their diffusion coefficient becomes much smaller than a usual surface diffusion coefficient. In this case T is small for sufficiently small values of θ' and consequently the rate constants K_{ij} are initially strongly dependent upon time [Eq. (3')]. For further clarification we represent in Fig. 18 the dimensionless rate constant $K_{11}/(4\pi D_{11})$ as a function of θ' for $D_{11} = 10^{-16}$ cm^2/sec and $R_{11} = 10^{-7}$ cm. One may observe a rapid variation until $\theta' \simeq 10^3$ sec, and a nearly constant value for $\theta' > 10^3$ sec. Only if the critical value $\theta'_c \simeq 10^3$ sec is small compared to the time t of the process it is reasonable to consider the rate constants independent of the small scale time θ'. In the cases

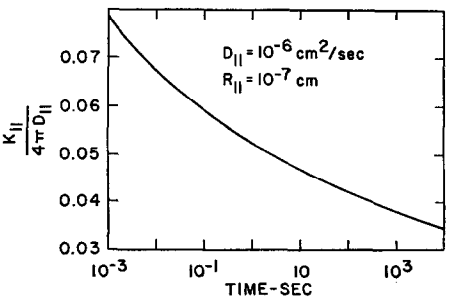

Fig. 17. Dimensionless rate constant in the diffusion controlled case vs time.

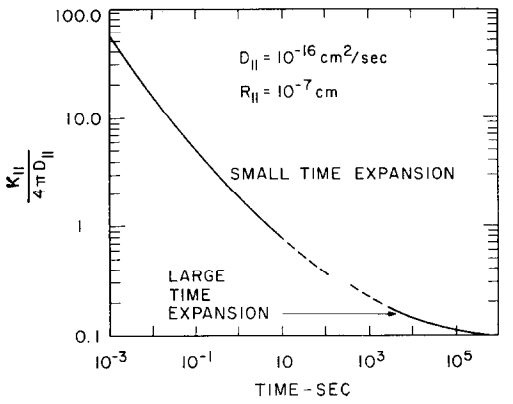

FIG. 18. Dimensionless rate constant in the diffusion controlled case vs time for decreased mobility.

considered here, the time of the process is larger by several orders of magnitude than the critical time.

The present approach can be used if θ' simultaneously satisfies the following conditions: (a) θ' is sufficiently long and as a consequence T large enough for equation (3‴) to be valid, (b) θ' is sufficiently small compared to the time in which an appreciable modification of the concentrations N_{v_k} occurs.

APPENDIX II. SIMILARITY THEORY FOR THE SIZE DISTRIBUTION OF THE SINTERING PROCESS (9)

The dimensionless groups used to account for the similarities in the shapes of the particle-size spectra at different times of the process, can be derived by means of a similarity solution.

First a continuous distribution function $n(v, t)$ is introduced such that $n(v, t)\,dv$ is the number of particles per unit surface area having a volume in the range v to $v + dv$. Equations (2) may be written in the form:

$$\frac{\partial n(v,t)}{\partial t} = \frac{1}{2}\int_0^v K(\tilde{v}, v-\tilde{v})n(\tilde{v},t)n(v-\tilde{v},t)\,d\tilde{v} - n(v,t)\int_0^\infty K(\tilde{v},v)n(\tilde{v},t)\,d\tilde{v} \quad \text{(II-1)}$$

The rate constants $K(\tilde{v}, v)$ are given for the two limiting cases of "diffusion control" and sintering control by Eqs. (3‴ and 4), respectively. If the size dependence of the diffusion coefficient D_{ij} and reaction rate constants for the merging process α_{ij} is taken into account as listed in Table 1, the rate constants $K(\tilde{v}, v)$ can be written as:

$$K(\tilde{v}, v) = K^*(\tilde{v}^m + v^m). \quad \text{(II-2)}$$

Here K^* is a constant and the exponent m depends on the mechanism and on the size dependence of either the diffusion coefficients or the reaction rate constants (see Table 1).

One may observe that the distribution function depends on two variables, v and t. The aim of the similarity solution is to find a change of variables, able to transform Eq. (II-1) into an ordinary integro-differential equation and thus to reduce the number of variables.

The similarity solution will be constructed by means of two parameters: the total number of particles per unit surface area of support $N(t)$, and the total volume of particles per unit area of support ϕ. This choice is arbitrary. Other moments of the distribution function $n(v, t)$, as for instance the total exposed surface area of metal, could be used as well. The results obtained would be equivalent.

$N(t)$ and ϕ are chosen because of their simple physical significance. They are given by

$$N(t) = \int_0^\infty n(v,t)\,dv \quad \text{(II-3)}$$

$$\phi = \int_0^\infty vn(v,t)\,dv. \quad \text{(II-4)}$$

New variables are now introduced

$$\eta = v/v^*(t) \quad \text{(II-5)}$$

and

$$n(v,t) = h(t)\psi(\eta), \quad \text{(II-6)}$$

where $h(t)$ and $v^*(t)$ are functions of time. The form of these functions is determined from Eqs. (II-3) and (II-4). Introducing Eqs. (II-5 and II-6) into (II-3 and II-4), one obtains

$$h(t) = \frac{B}{A^2}\frac{N^2}{\phi} \tag{II-7}$$

$$v^*(t) = \frac{A}{B}\frac{\phi}{N}, \tag{II-8}$$

where

$$A \equiv \int_0^\infty \psi(\eta)\, d\eta \tag{II-9}$$

and

$$B \equiv \int_0^\infty \eta\psi(\eta)\, d\eta \tag{II-10}$$

are universal constants. The similarity variables $\psi(\eta)$ and η, given by Eqs. (II-5 and II-6), can now be written as

$$\eta = \frac{B}{A}\frac{N(t)}{\phi} v \tag{II-5'}$$

$$n^* = \frac{\phi n(v,t)}{N(t)^2} = \psi(\eta)\frac{B}{A^2}. \tag{II-6'}$$

Such a type of similarity transformation was first suggested, in a different problem, by Friedlander (*34, 35*).

Before transforming Eq. (II-1) into an ordinary integro-differential equation, the rate of change of the total number of particles, $dN(t)/dt$, has to be known. By integrating Eq. (II-1) over all particle sizes one obtains

$$\frac{\partial}{\partial t}\int_0^\infty n(v,t)\, dv = \frac{dN(t)}{dt} = -\frac{K^*}{2}\int_0^\infty\int_0^\infty n(v,t)n(\tilde{v},t)\,[\tilde{v}^m + v^m]\, dv\, d\tilde{v}. \tag{II-11}$$

Inserting Eqs. (II-5' and II-6') into (II-11), yields

$$\frac{dN}{dt} = -b_1 N^{2-m}, \tag{II-12}$$

where

$$b_1 = \frac{K^*}{2}\phi^m \frac{A^{m-2}}{B^m}\int_0^\infty\int_0^\infty \times \psi(\eta)\psi(\tilde{\eta})(\eta^m + \tilde{\eta}^m)\, d\eta\, d\tilde{\eta}. \tag{II-13}$$

Equations (II-1), (II-2), (II-5'), (II-6'), and (II-12) lead to the following ordinary integro-differential equation

$$\left[2\psi(\eta) + \eta\frac{d\psi(\eta)}{d\eta}\right]\int_0^\infty\int_0^\infty \times \psi(\eta)\psi(\tilde{\eta})(\eta^m + \tilde{\eta}^m)\, d\eta\, d\tilde{\eta} + \int_0^\infty \psi(\eta)\, d\eta \int_0^\eta \times \psi(\tilde{\eta})\psi(\eta - \tilde{\eta})[\tilde{\eta}^m + (\eta - \tilde{\eta})^m]\, d\tilde{\eta} - 2\psi(\eta)\int_0^\infty \psi(\eta)\, d\eta \int_0^\infty \times \psi(\tilde{\eta})(\eta^m + \tilde{\eta}^m)\, d\tilde{\eta} = 0 \tag{II-14}$$

Of course the solution of Eq. (II-14) represents only one of the possible particular solutions of Eq. (II-1). The main problem is whether this particular solution which is compatible only with special types of initial conditions has physical meaning. In what follows an answer to this question is given. A solution of Eq. (II-14) in closed form was obtained only for constant K_{ij} [$m = 0$, Eq. (II-2)], namely

$$\psi(\eta) = e^{-\eta}. \tag{II-15}$$

For size dependent reaction rate constants the solution of Eq. (II-14) was obtained by replotting the numerical results of the discrete spectrum using the similarity variables. The similarity variables for the discrete case were taken as:

$$\eta^*_i = iv_1 N/\phi \tag{II-5''}$$

$$\psi^*(\eta^*_i) = N_{v_i}\phi/N^2 v_1 \tag{II-6''}$$

Figures 19 and 20 show the obtained results. For the "diffusion control" mechanism the numerical solution after a short time becomes independent of the initial distribution of sizes and can be represented after this short time by the similarity solution (Fig. 19). For "sintering control" a family of curves characterized by a supplementary dimensionless time τ_1, is obtained (Fig. 20). These curves are, however, close to each other. For this reason information concerning some cumulative distributions as are the total number of particles per unit surface area of support and the total exposed surface area of the metal may be obtained from the similarity transformation even in the sintering controlled case.

In what follows an equation for the decay of the exposed surface area of metal

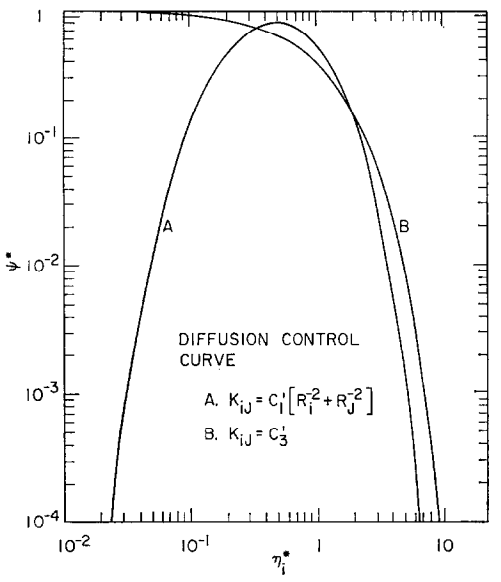

FIG. 19. Similarity solution for diffusion controlled cases.

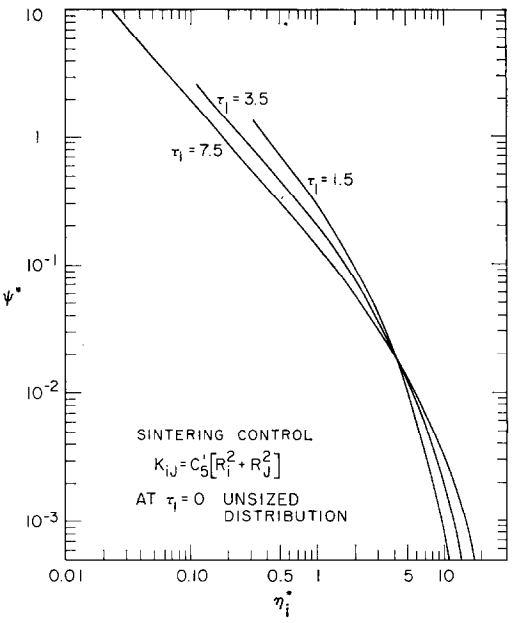

FIG. 20. Similarity solution for sintering controlled case.

is established using the similarity variables. A continuous formulation of the exposed surface area may be written as:

$$S(t) = b_2 \int_0^\infty v^{2/3}\, n(v,t)\, dv \quad \text{(II-18)}$$

where b_2 is a geometric factor, dependent on the shape of the particles. Introducing the similarity variables, Eqs. (II-5′) and (II-6′), into Eq. (II-18), one finds that the rate of decay of the exposed surface area of metal is given by:

$$\frac{dS(t)}{dt} = -b_3 S(t)^{4-3m}, \quad \text{(II-19)}$$

where

$$b_3 = \frac{K^*}{6\phi^{2-3m} A B^{3m-2} b_2^{3-3m}} \times \int_0^\infty \int_0^\infty \psi(\eta)\psi(\tilde{\eta})(\eta^m + \tilde{\eta}^m)\, d\eta\, d\tilde{\eta} \Big/ \left[\int_0^\infty \eta^{2/3}\psi(\eta)\, d\eta\right]^{3-3m} \cdot \quad \text{(II-20)}$$

Eq. (II-19) is equivalent to those established on the basis of numerical computations (see Table 1).

NOMENCLATURE

A	Universal constant defined by Eq. (II-9).
a	Actual area of the solid–solid interface of crystallite and support.
a_{ap}	Apparent area of the solid–solid interface of crystallite and support.
B	Universal constant defined by Eq. (II-10).
b_1, b_2, b_3	Constants in Eqs. (II-12), (II-18), and (II-19).
c	Concentration of the surface active metal within the metal crystallite.
C_i, C'_i, C''_i	Constants independent of time.
D_{ij}	Diffusion coefficient of particle i with respect to particle j.
$F_{v_{k,0}}$, F_{v_k}	Number of fixed particles per unit surface area of support composed of k metal units at $t = 0$, and $t = t$, respectively.
$h(t)$	Function of time defined by Eq. (II-7).

J_0	Bessel function of the first kind and zero order.
K, K_i	Rate constant independent of time.
K^*	Constant independent of particle size.
K_{ij}, K^*_{ij}	Second order rate constant used in the discrete representation.
$K(v, \tilde{v})$	Second order rate constant used in the continuous representation.
m	Exponent in Eq. (II-2).
N, N_0	Total number of particles per unit surface area of support for $t = t$ and $t = 0$, respectively.
$N_{v_{k,0}}, N_{v_k}$	Number of moving particles per unit surface area of support composed of k metal units at time $t = 0$ and $t = t$, respectively.
n	Exponent in Eq. (1).
$n(v, t)$	Continuous density distribution function.
p	Probability that a particle formed from two colliding moving particle will move.
q	Probability that a fixed particle will move after collided by a moving particle.
R	Universal gas constant.
R_{ij}	Radius of interaction between two colliding particles i and j.
$r = a/a_{ap}$	Wenzel's ratio, actual area of interface divided by apparent area of interface.
r_i	Radius of particle containing i metal atoms.
S	Total exposed surface area of the metal per unit surface area of support.
S_0	Value of S at the initial moment.
S_k	Exposed surface area of a particle containing k metal units.
$T = D_{ij}\theta'/R_{ij}^2$	Dimensionless time.
t	Time of the process.
$U_{ss'}$	Interaction energy per unit surface area between the atoms on one side of the interface and the atoms on the other side of the interface.
U_{str}	Strain plus dislocation or fracture energy per unit surface area.
u	Dummy variable.
v	Volume of a particle.
v_i	Volume of a particle containing i metal units.
$v^*(t)$	Function of time defined by Eq. (II-8).
W	Work of adhesion.
Y_0	Bessel function of the second kind and zero order.
α_{ij}	Reaction rate constant for the merging process of two particles containing i and j units.
β_k	Trapping rate constants.
Γ_{sg}	Surface excess concentration of the surface active impurity on the support–gas interface.
$\Gamma_{s'g}$	Surface excess concentration of the surface active impurity on the metal–gas interface.
$\Gamma_{ss'}$	Surface excess concentration of the surface active metal on the support–metal interface.
$\gamma = 0.5772$	Euler's constant.
χ	Spreading coefficient.
$\sigma_{sg}, \sigma_{s'g}$	Metal–gas surface tension and support–gas surface tension.
$\sigma_{ss'}$	Solid–solid surface tension.
η	Similarity variable in the continuous representation, dimensionless volume.
η^*_i	Similarity variable in the discrete representation.
θ	Contact angle.

θ' Small scale time in the diffusion model.

θ^* = 1 sec.

μ Chemical potential.

$\tau_1 = t\alpha_{11}2\pi R_1 N_0$ Dimensionless time in the sintering-controlled case.

$\tau_2 = \dfrac{t4\pi D_1 N_0}{\ln [4D_{11}\theta^*/(R_{11})^2]}$ Dimensionless time in the diffusion-controlled case.

ϕ Total volume of metal per unit surface area of support.

ψ Similarity variable in the continuous representation, dimensionless distribution function.

ψ^* Similarity variable in the discrete representation.

References

1. Maat, H. J., and Moscou, L., *Proc. 3rd Int. Congr. Catal.* **II**, 1277 (1965).
2. Zaidman, N. M., Dzisko, V. A., Karnautkhov, A. P., Kefeli, L. M., Krasilenko, N. P., Koroleva, N. G., and Ratner, I. D., *Kinet. Katal.* **10**, 386 (1969).
3. Gruber, H. L., *J. Phys. Chem.* **66**, 48 (1962).
4. Dorling, T. A., Lynch, W. J., and Moss, R. L., *J. Catal.* **20**, 190 (1971).
5. Mills, G. A., Weller, S., and Cornelius, E. B., *Proc. 2nd Int. Congr. Catal. Paris*, 2221 (1960).
6. Herrmann, R. A., Adler, S. F., Goldstein, M. S., and DeBaun, R. M., *J. Phys. Chem.* **65**, 2189 (1961).
7. Hughes, T. R., Houston, R. J., and Sieg, R. P., *Ind. Eng. Chem. (Proc. Des. Dev.)* **1**, 96 (1962).
8. Adler, S. F., and Keavney, J. J., *J. Phys. Chem.* **64**, 208 (1960).
9. Ruckenstein, E., and Pulvermacher, B., *AIChE Journal* **19** March, 1973.
10. Bassett, G. A., *in* "Proceedings of the European Regional Conference on Electron Microscopy" (A. L. Houwink and B. J. Spit, eds.), I, De Nederlandse Vereniging voor Elektronen microscopie, Delft (1960).
11. Bassett, G. A., *in* "Proceedings of the International Symposium on Condensation and Evaporation of Solids," (E. Rutner, P. Goldfinger, and J. P. Hirth, eds.), Gordon and Breach, New York (1964).
12. Skofronick, J. G., and Phillips, W. B., *J. Appl. Phys.* **38**, 4791 (1967).
13. Phillips, W. B., Desloge, E. A., and Skofronick, J. G., *J. Appl. Phys.* **39**, 3210 (1968).
14. Ries, H. E., "Advances in Catalysis" (W. G. Frankenburg, V. I. Komarewsky, and R. K. Rideal, eds.), IV, Academic Press, New York (1952).
15. Shapiro, I., and Kolthoff, I. M., *J. Amer. Chem. Soc.* **72**, 776 (1950).
16. Williams, A., Butler, G. A., and Hammonds, J., *J. Catal.* **24**, 352 (1972).
17. Smorjai, G. A., Powell, R. E., Montgomery, P. W., and Jura, G., *in* "Small-Angle X-Ray Scattering," (H. Brumberger, ed.), Gordon and Breach, New York (1965).
18. Geus, J. W., *in* "Chemisorption and Reactions on Metallic Films" (J. R. Anderson, ed.), Academic Press, London and New York (1971).
19. Bradshaw, F. J., Brandon, R. H., and Wheeler, C., *Acta Met.* **12**, 1057 (1964).
20. Zackay, V. F., Mitchell, D. W., Mitoff, S. P., and Pask, J. A., *J. Amer. Ceram. Soc.* **36**, 84 (1953).
21. Pask, J. A., and Fulrath, R. M., *J. Amer. Ceram. Soc.* **45**, 592 (1962).
22. Schäfer, H., and Tebben, A., *Z. Anorg. Allgem. Chem.* **304**, 317 (1960).
23. Raub, E., and Plate, W., *Z. Metallkunde* **48**, 529 (1957).
24. Fryburg, G. C., *Trans. Met. Soc. AIME* **233**, 1986 (1965).
25. Bartlett, R. W., *J. Electrochem. Soc.* **114**, 547 (1967).
26. Kern, R., Masson, A., and Métois, J. J., *Surface Sci.* **27**, 483 (1971).
27. Métois, J. J., Gauch, M., Masson, A., and Kern, R., *Surface Sci.* **30**, 43 (1972).
28. Wilson, G. R., and Hall, W. K., *J. Catal.* **17**, 190 (1970).
29. Wilson, G. R., and Hall, W. K., *J. Catal.* **24**, 306 (1972).
30. Sutton, H., and Feingold, E., *in* "Materials Science Research," (W. W. Kriegel and H. Palmour III, eds.), Vol. 3. Plenum Press, New York (1966).
31. Sinfelt, J. H., *Chem. Eng. News*, June 1972.
32. Kuczynski, G. C., *Trans. Met. Soc. AIME* **185**, 169 (1949).
33. Satterfield, C. N., "Mass Transfer in Heterogeneous Catalysis," M. I. T. Press, Cambridge, MA (1970).
34. Friedlander, S. K., *J. Meteorol.* **18**, 753 (1961).

35. SWIFT, D. L., AND FRIEDLANDER, S. K., *J. Colloid Sci.* **19,** 621 (1964).

36. JAWORSKA-GALAS, Z., WRZYSZCZ, J., *Int. Chem. Eng.* **6,** 604 (1966).

37. WELLER, S. W., AND MONTAGNA, A. A., *J. Catal.* **20,** 394 (1971).

38. JOHNSON, M. F. L., AND KEITH, C. D., *J. Phys. Chem.* **67,** 200 (1963).